JOURNAL of the MEXICAN CHEMICAL SOCIETY

https://www.jmcs.org.mx/

Article

Open Access

J. Mex. Chem. Soc. **2026**, *70(1):e2467*

Received March 29th, 2025
Accepted September 24th, 2025

http://dx.doi.org/10.29356/jmcs.v70i1.2467
e-location ID: 2467

Keywords:
Venturi tube; thymol; chitosan; nanoparticles; ionic gelation; mixer

Palabras clave:
Tubo Venturi; timol; quitosano; nanopartículas; gelación iónica; mezclado

***Corresponding author:**
García-Salazar, Gilberto
email: gilberto.gs@comunidad.unam.mx

ISSN-e 2594-0317

Thymol-Loaded Chitosan Nanoparticles: A New Ionic Gelation Method Using a Venturi Tube

García-Salazar, Gilberto[1], Romero-Alatorre, Diego Francisco[1], Zambrano-Zaragoza, María de la Luz[2], Serrano–Mora, Luis Eduardo[1], Vidal-Romero, Gustavo[3], Quintanar-Guerrero, David [1]

[1]Universidad Nacional Autónoma de México, Facultad de Estudios Superiores Cuautitlán, Laboratorio de Investigación y Posgrado en Tecnología Farmacéutica, Av. 1° de Mayo s/n Cuautitlán Izcalli, CP 54745, Estado de México, México.
[2]Universidad Nacional Autónoma de México, Facultad de Estudios Superiores Cuautitlán, Laboratorio de Procesos de Transformación de Alimentos y Tecnologías.
Emergentes, Km 2.5 Carretera Cuautitlán–Teoloyucan, San Sebastián Xhala, Cuautitlán Izcalli, CP 54714, Estado de México, México.
[3]Universidad Nacional Autónoma de México, Facultad de Estudios Superiores Zaragoza Campus II, Departamento de Tecnología Farmacéutica, CP 09230, Ciudad de México, México.

Abstract. This study aimed to explore the potential of the Venturi tube as an innovative and scalable platform for preparing thymol-loaded chitosan nanoparticles (Tym-Ch-NP´s) using the ionic gelation method. Chitosan and thymol was used as polymer and bioactive compound, respectively. Unlike conventional processes, the Venturi tube provides continuous and efficient mixing, enhancing mass transfer and process reproducibility, which are key challenges in nanoparticle production. The effects of recirculation rate, stabilizing and crosslinking agent concentrations were evaluated. The systems obtained showed particle size around of ~ 300 nm, polydispersity index ~ 0.3 and zeta potential ~ +30 mV. Encapsulation efficiency ranged from 18.5 to 67.5 %. The highest efficiency was obtained under the following conditions: stabilizer 3.0 % (w/v), tripolyphosphate 0.5 % (w/v) and recirculation rate 5.8 L/min. The transmission and backscattering profiles verified that the nanoparticles prepared showed slight flocculation, with a ΔBS < 10 %, but

J. Mex. Chem. Soc. **2026**, *70(1):e2467*
Regular Issue

ISSN-e 2594-0317

are considered stable due to their zeta potential. These findings highlight the novelty and importance of adapting the Venturi tube to ionic gelation, demonstrating its capacity to produce stable nanoparticles and include model drug with potential application in the pharmaceutical chemical industry in a reproducible and scalable manner.

Resumen. El principal objetivo de este estudio fue explorar el potencial del tubo Venturi como una plataforma innovadora y escalable en la preparación de nanopartículas de quitosano cargadas con timol usando el método de gelación iónica. Para este método se utilizó quitosano como polímero y timol como compuesto bioactivo. A diferencia de los sistemas convencionales por lote, el tubo Venturi proporciona una mezcla continua y eficiente, mejorando la transferencia de masa y la reproducibilidad del proceso, que representan desafíos clave en la producción de nanopartículas. Los resultados demostraron el efecto de la velocidad de recirculación, concentración del estabilizante y agente de entrecruzamiento. El tamaño de partícula obtenido fue de ~ 300 nm, el índice de polidispersidad de ~ 0.3 y el potencial zeta de ~ + 30 mV. La eficiencia de encapsulación fue de 18.5 a 67.5 %. La mejor eficiencia de encapsulación se obtuvo empelando: estabilizante al 3.0 % (p/v), tripolifosfato 0.5 % (p/v) y una velocidad de recirculación de 5.8 L/min. Los perfiles de retrodispersión de luz mostraron una leve floculación con un valor de ABS menor al 10 %, pero es considerado estable debido a su valor de potencial zeta. Estos hallazgos destacan la novedad e importancia de la adaptación de la metodología del tubo Venturi a la de gelación iónica, demostrando su capacidad para producir nanopartículas estables y encapsular compuestos bioactivos con potencial aplicación en la industria química farmacéutica de manera reproducible y escalable.

Introduction

Mixing the ingredients of macro and nanodisperse systems is generally performed in an individual apparatus using rotating parts, such as impellers or propellers, that mechanically agitate the fluids to promote random particle relocation [1]. This method typically involves batch processing that requires an external energy source. However, operations of this kind are intermittent, and final product yield is often low. Passive or static mixing is an alternative approach that utilizes devices with specific geometric designs to facilitate mechanical mixing and mass transfer. The Venturi tube is commonly used to produce disperse systems like polymeric and lipid nanoparticles. Our research group has conducted studies to evaluate the effectiveness of the Venturi tube as a static mixer for producing a disperse system [2,3]. Results suggest that this tube produces nanoparticles with good process efficiency.

Chitosan is known to have numerous applications in various fields, such as medicine, food, cosmetics, textiles, agriculture, and veterinary science [4], due to its structure, biocompatibility, biodegradability, and other specific functional properties. Polymeric nanoparticles can be prepared by various methods, including ionic gelation, emulsification, and simplex and complex coacervation [5]. Chitosan is a biopolymer widely used as a coating in the development of packaging systems because it protects substances due to its antioxidant and antimicrobial properties. Thus, studies have been conducted on encapsulating thymol –the largest component of thyme essential oil– which has shown antioxidant and antimicrobial potential for use as a natural additive in foods [6]. Recently, optimization of the encapsulation process with thymol chitosan was achieved with a maximum encapsulation efficiency of 67.1 % and particle sizes >300 nm (Çakır, Icyer and Tornuk, 2020).

Nanoparticles produced by ionic gelation are typically prepared using batch processing, but this method often requires high energy consumption, and produces irregular surface morphology, fragile particulate systems, and high indices of dispersibility [7]. Another method for producing polymeric nanoparticles utilizes the Venturi tube, a static mixer with several advantages: low energy consumption, small space requirements, low cost, and recirculation operations that enhance the mixing process.

The Venturi tube method for producing nanoparticles is also simple, quick, and efficient. The device's shape generates an exponential increase in contact between two liquids, allowing them to mix rapidly and more thoroughly. Its action produces a suction effect that further enhances contact between the liquids due to the high Reynolds number achieved via system recirculation. This system could also be used as a large-scale platform for nanoparticle production employing distinct procedures.

http://dx.doi.org/10.29356/jmcs.v70i1.2467

J. Mex. Chem. Soc. **2026**, *70(1):e2467*
Regular Issue

ISSN-e 2594-0317

The main aim of this study was to evaluate the efficiency of the Venturi tube in preparing thymol-loaded chitosan nanoparticles (Tym-Ch-NP´s) using Tween 80® as the stabilizing agent and tripolyphosphate as the crosslinking agent. The effects of the recirculation rate, the concentration of the stabilizing and crosslinking agents were analyzed on the key physicochemical characteristics of the nanoparticles: particle size, the polydispersity index (PDI), zeta potential (ZP), and encapsulation efficiency (EE), as well as stability test. Thymol, used as model bioactive compound was incorporated into the chitosan nanoparticles during the synthesis process for potential therapeutic application. Utilizing the Venturi tube represents a novel approach, particularly as a new method for ionic gelation improving its reproducibility.

Materials and methods

Materials

Low molecular weight chitosan (50,000-190,000 Da) with a deacetylation degree >75 %, Tween 80®, and Thymol (≥95 %) were purchased from Sigma-Aldrich, Mexico. Acetic acid, hydrochloric acid, and ethanol (95%) were purchased from Reactive Meyer, Mexico, while sodium tripolyphosphate (TPP) was obtained from Cosmopolitan, Mexico, and deionized water from the Millipore® Milli-Q water purification system.

Preparation of Tym-Ch-NP´s

The Tym-Ch-NP´s were synthesized using the Venturi tube method as described by García-Salazar et al. (2021), employing the ionic gelation method [8] with some modifications. On the one hand, a 0.3 % (w/v) chitosan solution was prepared using 1.0 % (v/v) acetic acid solution as dissolvent under magnetic stirring. This solution was filtered with a pore size of 2.5 µm and the pH was adjusted to 4.5 using phthalate buffer. On the other hand, 0.3 % (w/v), 0.5 % (w/v), and 1.0 % (w/v) solutions of TPP were prepared using deionized water.

The mixing process involved recirculating 150 mL of chitosan solution adjusted to pH 4.5 through the entire system using a pump (Brushless, VOVYO Technology Co., Ltd., China) varying the recirculation rate; 1.7 L/min, 3.6 L/min, and 5.8 L/min. Tween 80® at 1.0 % (w/v), 2.0 % (w/v), and 3.0 % (w/v) was added to a chitosan solution in the Venturi tube and the mixture was recirculated for 10 minutes to form an emulsion. After that, a solution of 10 mg/mL of thymol was injected into the system while the recirculation was in progress followed by injection of 55 mL of a TPP solution into the throat of the Venturi tube at a rate of 1.0 mL/min, controlling the infusion with a syringe pump (model NE-300, Pumps Systems, Inc., USA). The emulsion was mixed continuously for 30 min and the emulsion was collected and sieved through filter paper with a pore size of 2.5 µm. Finally, Tym-Ch-NP´s was collected by centrifugation at 6000 rpm for 1h at 5.0°C and the particles obtained were dispersed in distilled water (Fig. 1).

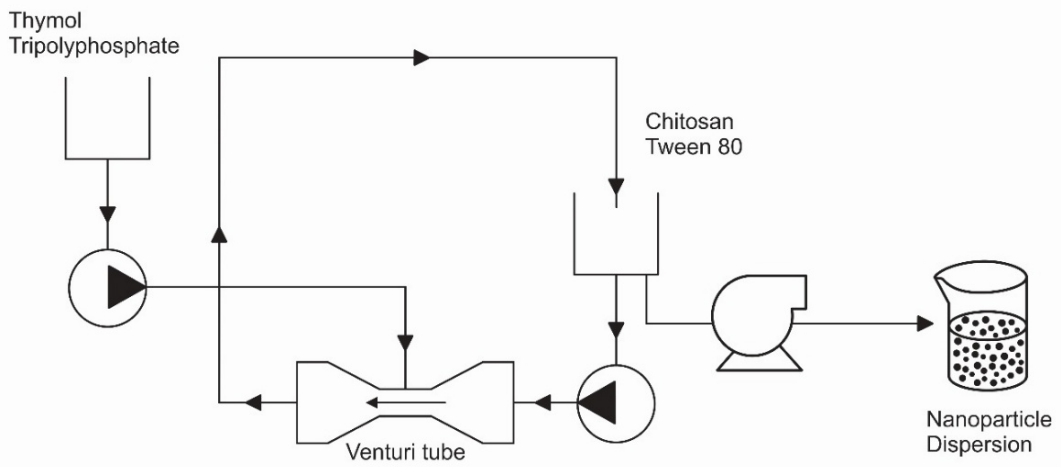

Fig. 1. Scheme of ionic gelation synthesis of chitosan nanoparticles by Venturi tube method.

http://dx.doi.org/10.29356/jmcs.v70i1.2467

J. Mex. Chem. Soc. **2026**, *70(1):e2467*
Regular Issue

ISSN-e 2594-0317

Characterization of the Tym-Ch-NP´s

Encapsulation efficiency (EE) of Tym-Ch-NP´s was determined by UV–Vis spectrophotometry. This analysis was performed at 25 °C, to avoid multiple scattering effects, after diluting the nanoparticles with Milli-Q water. All measurements were performed in triplicate.

Loading capacity and encapsulation efficiency

The loading capacity (LC) and encapsulation efficiency (EE) of *Tym-Ch-NP´s* ChNP were determined by UV-Vis spectrophotometry method. In this step, 5 mL of the nanoparticle dispersion were mixed with 5 mL of HCl 2.0 M and kept in a boiling water bath for 30 min. After cooling, 5 mL of ethanol were added to the mixture and allowed to dissolve for 5 min. That solution was centrifuged at 10,000 rpm for 5 min at 5 °C (Beckman, Optima, USA). The supernatant was collected and measured using a UV-vis spectrophotometer (Cary, Varian, USA) at a wavelength of 275 nm. The amount of thymol was calculated using a calibration curve of pure ethanol (R2=0.999). Each sample batch was measured in triplicate. Encapsulation efficiency (EE) was calculated using the following equation:

$$\mathrm{EE}(\%) = (\text{Weight of loaded compound}/\text{Weight of initial compound})\ \mathrm{X}\ 100$$

Stability test

Long-term stability

The particle size, PDI, and ZP values of the Tym-Ch-NP´s were measured at the following time intervals: zero hours, one week, two weeks, three weeks, and one month. Samples were maintained at 4 °C to ensure stability throughout storage.

Sample stability by a TurbisacanTM Classic MA 2000

Physical stability of the Tym-Ch-NP´s was evaluated using a Turbiscan Classic MA 2000 (Toulouse, France) equipped with a detection head that scans along the height of the sample while simultaneously acquiring transmission and backscattering data every 40 µm. The nanoparticle samples were scanned by an 880 nm near-infrared LED source. Transmission and backscattering signals were registered by detectors. 5 mL of each sample were placed in a cylindrical glass cell and placed in the Turbiscan at 25 °C. Readings were taken every 16 min for 48 h. Delta transmission and backscattering were used to assess stability.

Freeze-drying of the Tym-Ch-NP´s

The effectiveness of fructose, glucose and dextrose as cryoprotectants was evaluated by freeze-drying. The cryoprotectants at 5.0 % (w/v) were added to Tym-Ch-NP´s dispersions and the samples were freezing and then lyophilized for 48 h. To evaluate the re-dispersibility of the lyophilized samples, 20 mg of the resulting product were redispersed in 10 mL of water by shaking for 5 min. At that point, the mean diameter, PDI, and ZP were re-evaluated.

Results and discussion

Chitosan nanoparticles are typically prepared using conventional methods that usually involve mechanical agitation, such as Ultra Turrax. However, this results in a broad particle size distribution and only small amounts of nanoparticles [9,10]. These factors limit the usefulness of these nanoparticles for certain applications. Preparing chitosan nanoparticles by ionic gelation, meanwhile, usually requires a two-stage process. The first step requires forming an oil-in-water emulsion that includes chitosan, Tween 80®, and thymol. The second step consists in solidifying the droplets formed by ionic gelation of the chitosan with TPP [11].

Against this background, we developed a novel method for preparing chitosan nanoparticles using the Venturi tube, which allows fluids to mix rapidly. This mixer uses the momentum of the crossflow to create a suction effect that provides a high contact interface between two liquids due to the high Reynolds number achieved [12]. The turbulent flows produced generate a large interfacial surface area that improves the collision rate between two or more reactants [13]. To demonstrate the effectiveness of the Venturi tube, Tym-Ch-NP´s were prepared by ionic gelation with some modifications, as reported by Medina et al. (2019), Çakır et al. (2020), and Oluoch et al. (2021).

J. Mex. Chem. Soc. **2026**, *70(1):e2467*
Regular Issue

ISSN-e 2594-0317

Effect of the operating conditions on the preparation of the Tym-Ch-NP´s

Several batches of Tym-Ch-NP´s were prepared to evaluate the effect of the concentration of TPP and Tween 80® on the Venturi system's recirculation rate. The results, based on the response of particle size, PDI, and ZP, are shown in Table 1.

Influence of Tween 80® on the organic phase for preparing nanoparticles

Tym-Ch-NP´s at three different concentrations of Tween 80® 1.0, 2.0, and 3.0 % (w/v) were prepared at a constant recirculation rate of 5.8 L/min and a TPP concentration of 0.3 % (w/v). The results show that the concentration of Tween 80® had only a minimal impact on the particle size, PDI and ZP (Table 1). Masalova et al. (2013) similarly found no significant effect on particle size when using concentrations of Tween 80® that ranged from 0.5-5.0 %. Rajaram & Natham (2013) reported that the stabilizer Tween 80® is adsorbed onto the surface of nanoparticles, reducing the free surface energy that favors the stabilization of the nanoparticles formed. The PDI is a property used to describe the variation in the particle size of a population of a colloidal dispersion. A PDI value close to 1.0 has more than one population of particles, while a value near 0.0 indicates a single population [17]. The Tym-Ch-NP´s prepared in the Venturi tube had a PDI range of 0.2 to 0.3, which indicates that this method produced monodisperse nanoparticles. The ZP of the dispersions was positive, with an average value of +30 mV (Table 1). This value reflects the presence of the amino groups of chitosan [18]. ZP values $\geq \pm 30$ mV are indicative of a stable emulsion [19], so we can predict that our nanoparticles will remain stable for extended periods.

Effect of the recirculation rate on nanoparticle characterization

The nanoparticles prepared by the Venturi tube method had a nanometric size of ~300 nm. Observations showed that at a recirculation rate of 1.7 L/min the nanoparticles had a size of 310.0 ± 3.6 nm, as shown in Table 1. This slight increase is attributed to turbulence generated inside the Venturi tube that was insufficient to efficiently disperse the TPP in the chitosan solution. Increasing the recirculation rate generated greater turbulence which produced micro-vortices that produced smaller, nanometer-size droplets [2]. As evidenced by our results, a recirculation rate of 3.6 L/min led to the formation of smaller, nanometer-size globules compared to a recirculation rate of 1.7 L/min. However, very intense agitation of 5.8 L/min may delay the binding of TPP to the chitosan molecules, resulting in the formation of larger nanoparticles, the destruction of the repulsive forces between the particles, and possible aggregation [20].

Effect of the TPP concentration on the properties of the Tym-Ch-NP´s

Tym-Ch-NP´s were prepared at three concentrations of TPP 0.3, 0.5, and 1.0 % (w/v) while maintaining a constant percentage of Tween 80® at 3.0 % (w/v) and applying a recirculation rate of 5.8 L/min. The results obtained under these conditions are shown in Table 1. TPP is a crosslinking agent that can improve the mechanical strength of the gel formed by chitosan. Nanoparticle formation occurs only when a sufficient number of crosslinks form between chitosan and TPP [21]. A decrease in ZP was observed when the TPP concentration was increased from 0.3 to 0.5% (w/v), possibly attributable to the fact that the charges of the Tym-Ch-NP´s decreased as the TPP concentration increased, due to the neutralization of the protonated amino groups of chitosan by TPP anions [18]. When nanoparticles were prepared with 1.0% (w/v) of TPP, however, a precipitate formed due to an excess concentration of TPP that produced stoichiometry with the chitosan and led to the formation of a large number of complexes between these two components of the formulation [20].

Effect of the variables tested on the encapsulation efficiency of Tym-Ch-NP´s

The EE of Tym-Ch-NP´s at the different concentrations of Tween 80®, TPP and distinct recirculation rates are shown in Table 1. Since EE directly reflects the amount of thymol incorporated within the chitosan matrix, these results demonstrate not only nanoparticle formation but also efficient drug incorporation. Observations revealed that the increase in the 67.5 % concentration of Tween 80® led to a higher EE, showed in F1 and F2. This indicates that Tween 80® permits incorporating a larger amount of the drug into the dispersion. Also, an increase in TPP concentration improved EE, due to the higher number of ionic cross-linking sites stabilizing the chitosan–TPP network, thereby minimizing drug leakage. However, when TPP exceeded the optimal range, oversaturation occurred, neutralizing the protonated amino groups of chitosan. This phenomenon favored particle aggregation, and, in some cases, precipitation [22] as noticed in F7. We further observed that the increase EE was strongly influenced by both the recirculation rate and the TPP concentration,

J. Mex. Chem. Soc. **2026**, *70(1):e2467*
Regular Issue

ISSN-e 2594-0317

due to the increased turbulence within the Venturi tube improved mixing efficiency which in turn provided a larger total surface area for chitosan-TPP interactions. This higher collision rate between chitosan chains and crosslinker molecules favored more effective entrapment of thymol within the polymer matrix, thereby increasing the EE that facilitated the incorporation of all the components necessary for nanoparticle formation.

In this study, the observed influence of TPP concentration and recirculation rate on EE demonstrates that the Venturi tube does not only affect nanoparticle size and stability but also significantly modulates the amount of thymol entrapped within the chitosan matrix. Thus, the method impacts both the physicochemical characteristics of the nanoparticles and their efficient drug incorporation. The optimized formulation obtained through Venturi-assisted ionic gelation (stabilizer 3.0% w/v, TPP 0.5% w/v, and recirculation rate of 5.8 L/min) achieved the highest thymol loading efficiency of 67.5 % confirming that the system is effectiveness in producing Tym-Ch-NP´s with desirable characteristic, including particle size ~300 nm, IP close to 0.0, and ZP around + 30 mV.

Table 1. Effect of the stabilizer, TPP, and recirculation rate on the characterization of the Tym-Ch-NP´s.

	Stabilizer (%) (w/v)	**TPP % (w/v)**	**Recirculation rate (L/min)**	**Particle size (nm)**	**PDI**	**ZP (mV)**	**Encapsulation efficiency %**
F1	1.0	0.3	5.8	317.7 ± 5.3	0.3 ± 0.02	32.1 ± 4.3	18.5 ± 0.6
F2	2.0	0.3	5.8	311.6 ± 4.8	0.2 ± 0.02	29.9 ± 3.5	34.9 ± 1.1
F3	3.0	0.3	5.8	286.0 ± 4.8	0.2 ± 0.01	30.7 ± 1.1	37.5 ± 0.2
F4	3.0	0.3	1.7	310.0 ± 3.6	0.3 ± 0.10	28.0 ± 1.3	48.7 ± 0.4
F5	3.0	0.3	3.6	239.7 ± 6.2	0.3 ± 0.02	33.6 ± 1.9	52.3 ± 0.1
F6	3.0	0.5	5.8	305.5 ±7.4	0.2 ± 0.01	25.0 ±0.3	67.5 ± 4.2
F7	3.0	1.0	5.8	NR	NR	NR	NR

Stability tests

The stability of the Tym-Ch-NP´s at 1.0, 2.0, and 3.0 % (w/v) of Tween 80® was monitored for 28 days at 4.0°C. These samples showed good stability, though a slight change in particle size was observed at the end of the monitoring period, as depicted in Fig. 2. This change may be attributable to the adhesive properties of chitosan nanoparticles, which can cause agglomerations when stored in an aqueous medium [23].

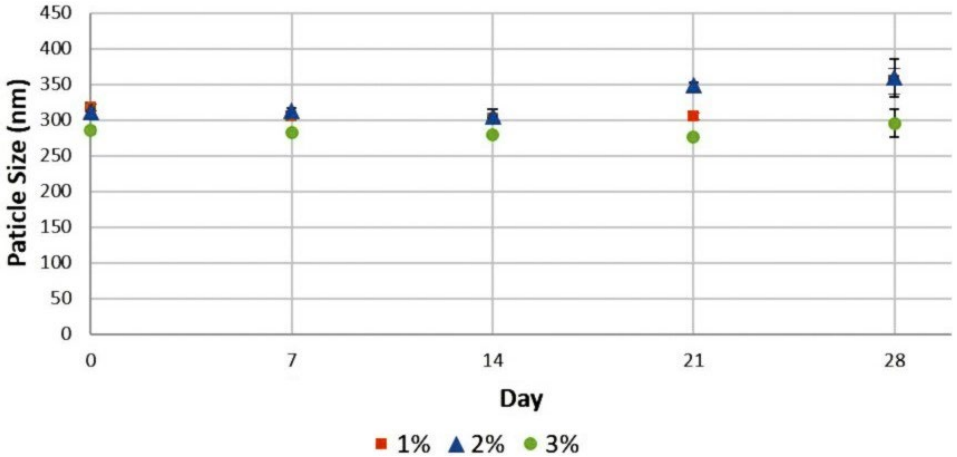

Fig. 2. Particle size of the Tym-Ch-NP´s with Tween 80® at 1.0, 2.0, and 3.0 % (w/v), TPP at 0.3 % (w/v) and a recirculation rate of 5.8 L/min.

http://dx.doi.org/10.29356/jmcs.v70i1.2467

J. Mex. Chem. Soc. **2026**, *70(1):e2467*
Regular Issue

ISSN-e 2594-0317

Effect of cryoprotectants on the characterization of the Tym-Ch-NP´s

Lyophilization, a form of freeze-drying, is often employed to preserve products in the food, medicine, cosmetic, and agricultural industries, and in veterinary science, among other fields. Cryoprotective agents like sugars, starches, and celluloses may be added to prevent particle aggregation and collapse during lyophilization [24]. In our study, various sugars, including fructose, glucose, and dextrose, were utilized as cryoprotectants to assess their effects on the results of lyophilization. The related findings for particle size, PDI, and ZP are shown in Table 2. Interestingly, nanoparticles subjected to sonication for 10 min experienced a slight decrease in size, likely due to fragmentation of large particles and agglomerates. However, the nanoparticles treated with fructose and dextrose exhibited a slight increase in size (~20.0 nm) that contrasted to the decrease (~20 nm) recorded when anhydrous glucose was added. This discrepancy could be due to variations in the efficiency of sonication among the distinct sugar formulations. Sonication, which is employed to disrupt nanoparticle agglomeration, resulted in a reduction in the number of large particles and an increase in smaller ones [25].

Measuring the ZP is a valuable method for evaluating the surface state of nanoparticles and detecting any modification post-lyophilization. A decrease in ZP after lyophilization, from ~30.0 to ~20.0 mV was observed, this can be attributable to a masking effect of the cryoprotective agent on the particle surface due to hydrogen bonding between the hydroxyl groups and the surface [26]. This phenomenon suggests that the cryoprotectant forms a protective layer on nanoparticles that may potentially affect their stability or functionality. We assume that hydrogen bonding occurs between the hydroxyl groups of the cryoprotective agent and the amino group of the chitosan. The primary focus of the stability assays was to evaluate the general influence of different sugars on particle size, polydispersity, and surface charge after lyophilization, rather than to maximize thymol retention. While fructose, glucose, and dextrose were effective in mitigating aggregation and size increase during freeze-drying, these experiments were conducted on representative nanoparticle batches and not exclusively on the formulation with the highest EE values (stabilizer 3.0 % w/v, TPP 0.5 % w/v, and recirculation rate 5.8 L/min). This decision was based on methodological considerations, as screening the effects of cryoprotectants required testing across different formulations to identify generalizable trends.

Table 2. Characterization of the Tym-Ch-NP´s after freeze-drying.

	Cryoprotector 5.0 % (w/v)	**Stabilizer % (w/v)**	**TPP % (w/v)**	**Recirculation rate (L/min)**	**Particle size (nm)**	**PDI**	**ZP (mV)**
F1	Fructose	1.0	0.3	5.8	331.8 ± 9.8	0.3 ± 0.03	21.2 ± 0.5
F2	Glucose	2.0	0.3	5.8	286.4 ± 2.1	0.4 ± 0.02	21.9 ± 0.9
F3	Glucose	3.0	0.3	5.8	271.4 ± 8.7	0.4 ± 0.02	22.6 ± 0.7
F4	Glucose	3.0	0.3	1.7	297.3 ± 3.5	0.3 ± 0.03	17.9 ± 0.6
F5	Dextrose	3.0	0.3	3.6	257.2 ± 5.3	0.4 ± 0.01	24.7 ± 0.6

The nanoparticles prepared under different operating conditions exhibited narrow particle size distributions (PDI 0.2 to 0.3) and stable positive zeta potentials (~ + 20 mV). These findings indicate that Venturi tube produces homogeneous nanoparticles across multiple batches, minimizing variability compared to conventional stirring-based methods. This reproducibility is particularly relevant for future scale-up and pharmaceutical applications, where batch-to-batch consistency is critical.

Turbiscan stability

To evaluate the stability of the nanoparticle dispersion, the ZP is generally measured as a reference parameter, with values below –30 mV or above +30 mV often indicating stable dispersions [19]. This parameter, however, does not provide information on the behavior of the formulation over time when phenomena like flocculation and coalescence can affect the homogeneity of a dispersion. Other techniques, such as turbiscan,

J. Mex. Chem. Soc. **2026**, *70(1):e2467*
Regular Issue

ISSN-e 2594-0317

can verify the stability of dispersions in real time based on optical properties [27] by detecting changes in transmission and backscattering as a function of particle movement in the dispersion [28]. By analyzing these optical properties, turbiscan can identify mechanisms of instability like sedimentation, cremation, flocculation, and coalescence.

As Fig. 3 shows, the transmission and backscattering plots for the Tym-Ch-NP´s prepared with Tween 80® at 3.0 % (w/v), a recirculation rate of 3.6 L/min, and TPP at 0.3% w/v (F5) did not reveal any significant differences. The profile remained at 5 % after 48 h with a constant vial height of 10-45 mm, indicating high physical stability during storage, without particle aggregation or flocculation of the nanoparticles. This degree of physical stability may be related to the ZP values >30 mV. However, for nanoparticles prepared under the conditions –Tween 80®, 2.0 % (w/v), recirculation rate, 5.8 L/min, and TPP at 0.3 % (w/v)– a 10 % profile was observed that suggested a slight flocculation and a slight increase in particle size [29]. This phenomenon can be explained by the fact that stored emulsions remain stable, but tend to aggregate due to hydrophobic attractions and van der Waals interactions, when the electrostatic repulsions are insufficient to overcome the forces of attraction [30]. However, a profile <10 % still demonstrates good physical stability, as can be corroborated by the ZP values for F3 (30.7 ± 1.1 mV) and F2 (29.9 ± 3.5 mV) [31].

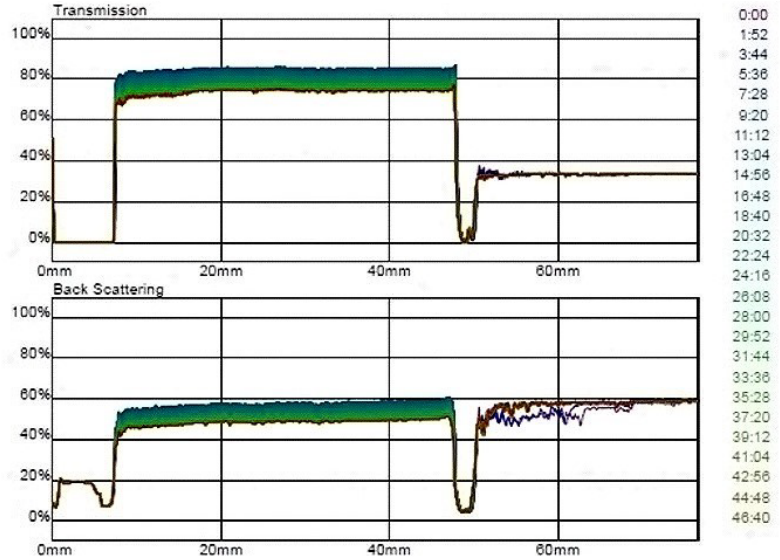

Fig. 3. Transmission and backscattering profile for F2 (Tween 80® at 2.0 % (w/v), recirculation rate, 5.8 L/min, and TPP at 0.3 % (w/v)), and F5 (Tween 80® at 3.0 % (w/v), recirculation rate, 3.6 L/min, and TPP at 0.3 % (w/v)).

Conclusions

In this study, Tym-Ch-NP´s were prepared successfully by implementing the ionic gelation technique in a Venturi tube. The shape of this tube generated internal turbulence that resulted in a high mixing rate which facilitated achieving our experimental objectives. The encapsulation efficiency values (18.5–67.5 %) reflected thymol incorporation, demonstrating that the Venturi tube influences not only nanoparticle size and stability but also efficient drug incorporation of the chitosan matrix. Optimal nanoparticles characteristics were achieved at a Tween 80® concentration of 3.0 % (w/v), a recirculation rate of 5.8 L/min, and a TPP concentration of 0.5 % (w/v). Under these conditions, the system yielded the highest thymol efficiency encapsulation (67.5 %) with a particle size of 305.5 nm, a PDI of 0.2, and ZP +25.6 mV. This findings highlight not only the feasibility and novelty of adapting the Venturi tube to ionic gelation but also its reproducibility. The method of Venturi tube produces nanoparticles with homogeneous size, stable surface charge, and tunable encapsulation efficiency under controlled conditions, indicating strong potential for industrial translation. This research demonstrates the versatility of the Venturi tube method as an effective platform for chitosan nanoparticle production via ionic gelation.

http://dx.doi.org/10.29356/jmcs.v70i1.2467

ISSN-e 2594-0317

References

1. Grzywacz, R. *Czas. Tech.* **2017**, *11*, 95–106. DOI: https://doi.org/10.4467/2353737xct.17.192.7421.
2. García-Salazar, G.; Zambrano-Zaragoza, M. L.; Quintanar-Guerrero, D. *Int. J. Pharm.* **2018**, *545*, 254–260. DOI: https://doi.org/10.1016/j.ijpharm.2018.05.005.
3. García-Salazar, G.; Zambrano-Zaragoza, M. de la L.; Serrano-Mora, E.; Mendoza-Díaz, S. O.; Leyva-Gomez, G.; Quintanar-Guerrero, D. *Drug Dev. Ind. Pharm.* **2021**, *47*, 1302–1309. DOI: https://doi.org/10.1080/03639045.2021.1989456.
4. Morin-Crini, N.; Lichtfouse, E.; Torri, G.; Crini, G. *Environ. Chem. Lett.* **2019**, *17*, 1667–1692. DOI: https://doi.org/10.1007/s10311-019-00904-x.
5. Singh, A.; Mittal, A.; Benjakul, S. *ScienceAsia*. **2021**, *47*, 1–10. DOI: https://doi.org/10.2306/scienceasia1513-1874.2021.020.
6. Llana-Ruiz-Cabello, M.; Pichardo, S.; Maisanaba, S.; Puerto, M.; Prieto, A. I.; Gutiérrez-Praena, D.; Jos, A.; Cameán, A. M. *Food Chem. Toxicol.* **2015**, *81*, 9–27. DOI: https://doi.org/10.1016/j.fct.2015.03.030.
7. Kunjachan, S.; Jose, S. *Asian J. Pharm.* **2010**, *4*, 148–153. DOI: https://doi.org/10.4103/0973-8398.68467.
8. Çakır, M. A.; Icyer, N. C.; Tornuk, F. *Int. J. Biol. Macromol.* **2020**, *151*, 230–238. DOI: https://doi.org/10.1016/j.ijbiomac.2020.02.096.
9. Oluoch, G.; Matiru, V.; Mamati, E. G.; Nyongesa, M. *Adv. Microbiol.* **2021**, *11*, 723–739. DOI: https://doi.org/10.4236/aim.2021.1112052.
10. Sullivan, D. J.; Cruz-Romero, M.; Collins, T.; Cummins, E.; Kerry, J. P.; Morris, M. A. *Food Hydrocoll.* **2018**, *83*, 355–364. DOI: https://doi.org/10.1016/j.foodhyd.2018.05.010.
11. Yoksan, R.; Jirawutthiwongchai, J.; Arpo, K. *Colloids Surf., B*. **2010**, *76*, 292–297. DOI: https://doi.org/10.1016/j.colsurfb.2009.11.007.
12. Sundararaj, S.; Selladurai, V. *Arab. J. Sci. Eng*. **2013**, *38*, 3563–3573. DOI: https://doi.org/10.1007/s13369-013-0643-9.
13. Shayeganfar, F.; Javidpour, L.; Taghavinia, N.; Tabar, M. R. R.; Sahimi, M.; Bagheri-Tar, F. *Phys. Rev.* **2010**, *81*, 026304-8. DOI: https://doi.org/10.1103/PhysRevE.81.026304..
14. Medina, E.; Caro, N.; Abugoch, L.; Gamboa, A.; Díaz-Dosque, M.; Tapia, C. *J. Food Eng.* **2019**, *240*, 191–198. DOI: https://doi.org/10.1016/j.jfoodeng.2018.07.023.
15. Masalova, O.; Kulikouskaya, V.; Shutava, T.; Agabekov, V. *Phys. Procedia*. **2013**, *40*, 69–75. DOI: https://doi.org/10.1016/j.phpro.2012.12.010.
16. Rajaram, S.; Natham, R. *Res. J. Pharm. Biol. Chem. Sci.* **2013**, *4*, 820–832.
17. Danaei, M.; Dehghankhold, M.; Ataei, S.; Hasanzadeh Davarani, F.; Javanmard, R.; Dokhani, A.; Khorasani, S.; Mozafari, M. R. *Pharmaceutics*. **2018**, *10*. DOI: https://doi.org/10.3390/pharmaceutics10020057.
18. Al-Nemrawi, N. K.; Alsharif, S. S. M.; Dave, R. H. *Int. J. Appl. Pharm.* **2018**, *10*, 60–65. DOI: https://doi.org/10.22159/ijap.2018v10i5.26375.
19. Escalona-Rayo, O.; Fuentes-Vázquez, P.; Jardon-Xicotencatl, S.; García-Tovar, C. G.; Mendoza-Elvira, S.; Quintanar-Guerrero, D. *J. Drug Deliv. Sci. Technol.* **2019**, *52*, 488–499. DOI: https://doi.org/10.1016/j.jddst.2019.05.026.
20. Algharib, S. A.; Dawood, A.; Zhou, K.; Chen, D.; Li, C.; Meng, K.; Zhang, A.; Luo, W.; Ahmed, S.; Huang, L.; et al. *J. Mol. Struct.* **2022**, *1252*, 132129. DOI: https://doi.org/10.1016/j.molstruc.2021.132129.
21. Bangun, H.; Tandiono, S.; Arianto, A. *J. Appl. Pharm. Sci.* **2018**, *8*, 147–156. DOI: https://doi.org/10.7324/JAPS.2018.81217.
22. Essid, R.; Ayed, A.; Djebali, K.; Saad, H.; Srasra, M.; Othmani, Y.; Fares, N.; Jallouli, S.; Abid, I.; Rashed, M.; et al. *Molecules*. **2023**, *28*, 5681. DOI: https://doi.org/10.3390/molecules28155681.
23. Gokce, Y.; Cengiz, B.; Yildiz, N.; Calimli, A.; Aktas, Z. *Colloids Surfaces A.* **2014**, *462*, 75–81. DOI: https://doi.org/10.1016/j.colsurfa.2014.08.028.

J. Mex. Chem. Soc. **2026**, *70(1):e2467*
Regular Issue

ISSN-e 2594-0317

24. Boge, L.; Västberg, A.; Umerska, A.; Bysell, H.; Eriksson, J.; Edwards, K.; Millqvist-Fureby, A.; Andersson, M. *J. Colloid Interface Sci.* **2018**, *522*, 126–135. DOI: https://doi.org/10.1016/j.jcis.2018.03.062.
25. Fernandez-De arlas, B.; Gómez, S.; Corcuera, M.-A.; Eceiza, A. *Rev. Iberoam. Polim.* **2014**, *15*, 211–218.
26. de Chasteigner, S.; Cavé, G.; Fessi, H.; Devissaguet, J.-P.; Puisieus, F. *Drug Dev. Res.* **1996**, *38*, 116–124.
27. Raikos, V. *Food Hydrocoll.* **2017**, *72*, 155–162. DOI: https://doi.org/10.1016/j.foodhyd.2017.05.027.
28. Kaombe, D. D.; Lenes, M.; Toven, K.; Glomm, W. R. *Energy Fuels*. **2013**, *27*, 1446–1452. DOI: https://doi.org/10.1021/ef302121r.
29. Mengual, O.; Meunier, G.; Cayré, I.; Puech, K.; Snabre, P. *Talanta*. **1999**, *50*, 445–456. DOI: https://doi.org/10.1016/S0039-9140(99)00129-0.
30. González-Reza, R. M.; Quintanar-Guerrero, D.; Del Real-López, A.; Piñon-Segundo, E.; Zambrano-Zaragoza, M. L. *LWT - Food Sci. Technol.* **2018**, *90*, 354–361. DOI: https://doi.org/10.1016/j.lwt.2017.12.044.
31. Santonocito, D.; Sarpietro, M. G.; Carbone, C.; Panico, A.; Campisi, A.; Siciliano, E. A.; Sposito, G.; Castelli, F.; Puglia, C. *Molecules*. **2020**, *25*. DOI: https://doi.org/10.3390/molecules25132991.